SIMULATION OF AN IRIS-GUIDED INVERSE FREE-ELECTRON LASER MICRO-BUNCHING EXPERIMENT

J. Frederico, G. Gatti, S. Reiche, J. Rosenzweig, R. Tikhoplav
UCLA, Los Angeles, CA 90095, USA

Abstract

This paper presents a detailed computational examination of various physical effects that enter into an innovative approach to inverse free-electron laser (IFEL) acceleration and microbunching experiments, involving use of irises to guide the high power laser beam.

In IFELs, there is a great advantage to using long wavelength, and thus diffractive lasers, which are also quite high power. As this scenario presents challenges to the final focusing optics, one must consider guiding, which for present schemes is either too lossy (in metallic guides), or incapable of supporting high fields (as in dielectric guides). Hence we are driven to examine an alternative scheme, that of using the effects of diffraction off of periodically placed metallic irises which have an inner diameter in a relatively low field region. We present below a computational analysis of the wave dynamics associated with the laser beam in this scheme. We then proceed to integrate this type of circularly polarized electromagnetic radiation field into a self-consistent simulation of beam dynamics inside of a helical undulator under construction at the UCLA Neptune Laboratory inverse free-electron laser. With this integrated tool, we then study the degree of microbunching bunching at the laser optical wavelength induced in a relativistic electron beam. Finally, we study the propagation of the beam after the IFEL interaction, including beam self-force (single component plasma) effects, to predict the level of microbunching at the fundamental (laser) frequency and its harmonics that are observed at a detector using coherent transition radiation.

INTRODUCTION

There are broad applications of a tunable coherent radiation source, ranging from medical uses to materials research and more. Current laser technology is not always completely tunable in terms of wavelength and generally has limits on achievable power. The free-electron laser (FEL) presents a solution in the form of a laser that can be tuned from centimeter wavelengths to the UV range [1]. The FEL also shows promise in the hard x-ray range compared to other approaches [2]. A bunched electron beam is a by-product of the FEL process, but can also be formed by a partial application of the process which is known as the inverse free-electron laser (IFEL).

For a FEL/IFEL application to be practical, it must be efficient. At longer wavelengths, diffraction causes a reduction in intensity at the electron beam, which must be

addressed. In particular, the longer the FEL is, the more the diffractive effects accumulate. A guide is an inviting solution; however, typical waveguides such as dielectric or metallic guides have inherent limitations concerning high-power radiation. In particular, dielectrics suffer material breakdown due to high fields especially near the center of the radiation field. Metallic guides rely on conductive boundary conditions to guide radiation, so at high power the walls are a source of strong resistive losses.

An iris-loaded guide, however, introduces physical structures in relatively low field regions [3]. The objective is to greatly reduce diffractive losses by sacrificing smaller power losses. However, physical trial and error to determine optimal operating parameters is impractical due to factors such as construction and installation. Computer simulation of the FEL process can provide insights into operating conditions under different scenarios.

EXPERIMENT

Experimental Set-up

The experiment simulated focuses on an IFEL application. The scheme to achieve bunching is a 10-cm IFEL section with included waveguide followed by a 30-cm drift section. The IFEL introduces electron beam energy modulation without significantly affecting bunching. The drift section converts energy modulation to bunching. The bunch period length is given by $2\pi/(k + k_U) = 10.5923\,\mu$m.

Standard IFEL. The IFEL section is a typical helical undulator configuration with the iris-loaded waveguide. The undulator satisfies the resonant condition in order to couple the electron beam to the radiation field [1]. The following equations [1] can be integrated to show energy and position modulation:

$$z = c\beta_0 t + z_0 \tag{1}$$

$$\dot{\gamma} = \frac{eE_0 K}{mc\gamma} \sin\left[(k + k_u)\,z - \omega t\right] \tag{2}$$

where $\beta_0 = \left[1 - \left(1 + K^2/2\right)/\gamma^2\right]^{1/2}$. The result is a sinusoidal energy modulation with no change in longitudinal particle position.

Iris-loaded Waveguide. The iris-loaded waveguide is within the undulator. In this region, the IFEL is designed

02 Synchrotron Light Sources and FELs

A06 Free Electron Lasers

to have an input radiation field that is orders of magnitude greater than the spontaneous radiation of the electrons; electron radiation is then overwhelmed by the input radiation. Since a Gaussian radiation field is fed into the iris waveguide and matched into its fundamental mode, a good approximation is that of the power contributing entirely to the fundamental mode. The power of the fundamental mode is then given by the power transmission of a Gaussian beam through the radius a of the iris apertures.

For a Gaussian beam, which would be the diffraction situation present in a standard IFEL, power transmission through a circular area of radius r is [4]:

$$T_{gauss}(r, z) = 1 - e^{-2r^2/w(z)^2} \qquad (3)$$

where $\omega(z) = w_0\sqrt{1 + (z/z_R)^2}$ and $z_R \equiv (\pi w^2)/\lambda$. Power transmission of free-space must be compared to that of an iris-loaded waveguide. A simple approximation is to consider only the power transmission in free space through the space defined by the geometry of the waveguide. As the radius of the waveguide is a, this power transmission is given by $T_{gauss}(a, z)$.

An iris-loaded waveguide is a regularly-spaced series of irises. Xie studied the second mode for Gaussian radiation [3]. This application is of the fundamental mode, and so the Bessel function of interest is J_0, and its zeroes, ν_{0n}. This change does not affect the theory, and can be applied to our configuration. Power flow through these series of apertures is

$$T_{iris}(z) = e^{-2\alpha_r z} \qquad (4)$$

where $\alpha_r \equiv [4\nu_{0n}^2\eta(M+\eta)]/L[(M+\eta)^2+\eta]^2$, ν_{0n} is the nth zero of the Bessel function J_0, or $J_0(\nu_{0n}) = 0$; $M = \sqrt{8\pi N}$; $N = a^2/\lambda L$; $\eta = -\xi(1/2)/\sqrt{\pi} \approx 0.824$, $\xi(z)$ is Riemann's Zeta function; and a is the aperture radius, L is the distance between apertures, and λ is the radiation wavelength. (Note that $\alpha_r(a, L, \lambda)$, and that a valid approximation for the scenario is only considering the dominant mode $n = 1$ for small diffraction loss $N \ll 1$.) [3] The waist of the radiation is matched to the iris aperture radius, such that $a \approx 3.23w/2$, so $T_{iris}(0) = T_{gauss}(\pi w_0/2, 0) = 1 - e^{-\pi^2/2} \approx 0.9928$. It is then possible to calculate the power transmission for a given distance z, $T_{iris}(z) = 0.9928e^{-2\alpha_r z}$.

Comparing the two power transmissions $T_{gauss}(\pi \omega_0/2, z)$ and $T_{iris}(z)$ using experimental parameters (see Table 1) yields Fig. 1. This view of transmission is, of course, incomplete. Especially in the beginning, the Gaussian wave cannot be perfectly matched into the main mode of the iris waveguide. A close examination would show that the dashed iris transmission is not continuous, as power is trimmed at irises and not continuously. However, as transmission differences increase, these details become negligible. It
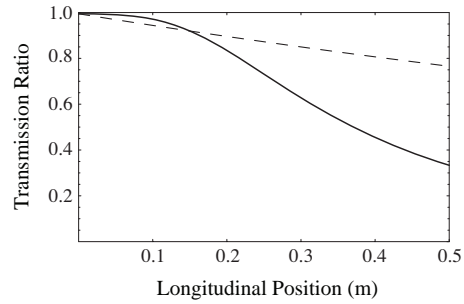
Figure 1: Transmission of power in free-space (solid) and iris waveguide (dashed)
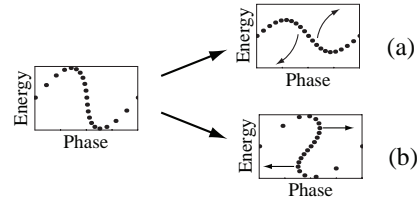

Figure 2: (a) Space charge effects dominate. (b) Space charge effects negligible

is expected, for our undulator that is only 0.1 m, that an iris IFEL should be nearly the same as a standard IFEL. It should also be noted that for a longer undulator, power transmission is significantly greater with an iris waveguide when compared to free-space propagation.

Drift Section. The dynamics in the drift section are influenced by space charge and can be described as a plasma oscillation of the electron beam.

For relatively low power, in the region where space charge is a significant factor, particles in phase space will be unable to fold over or over-compress. Electrons at the back of the bunch will lose energy as they are repulsed by electrons ahead of them, and similarly electrons at the front will gain energy as they are repulsed by those behind them. After reaching a maximum compression, bunches will spread out again. (See Fig. 2a.)

For negligible space charge, electrons will not interact with each other. The phase space will fold over (over-compress) and after maximum bunching, will spread out. (See Fig. 2b.) Maximum bunching would then be expected at the boundary between over-compression and under-compression.

In either scenario, modeled as a plasma, the distance $\lambda_p/2 = \pi/k_p$ to reach maximum bunching can be determined and is $k_p = \sqrt{4\pi r_e n_e/\beta^2\gamma^3}$ where $r_e = 2.8 \times 10^{-15}$ m, $n_e = I/(ec2\pi\sigma_x\sigma_y)$, σ_x and σ_y are the rms sizes of the electron beam, β is the beam velocity which can be solved from γ, and of course γ is given [5]. After manipulation, $\lambda_p/2 = 1.22$ m for given conditions and a current of 45 amps. It is worthwhile to note that $\lambda_p \propto I^{-1/2}$.

Genesis 1.3 was used to simulate the experiment [6]. The

Table 1: Experiment Parameters.

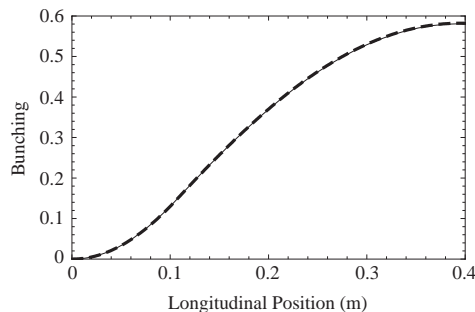| Radiation	
Wavelength (λ_r)	10.6×10^{-6} m
Intensity (I)	6×10^{11} W/cm^2
Peak E-field (E_0)	1.94×10^9 N/C
Waist (w_0)	0.7 mm
Electron Beam	
Energy (γ_0)	26.3
Current	45-1005 amps
Space Charge	First-order
Undulator	
Constant (K_u)	0.0940
Period (λ_u)	14.6 mm
Length	10 cm
Iris Guide	
Aperture Radius	1.13×10^{-3} m
Period	3 mm
Drift Section	
Length	30 cm

Figure 3: Simulated bunching as a function of position. 45 amps, 1.670304×10^8 watts. Dashed line indicates iris-loaded guide, thin line is standard.

code was modified to periodically remove radiation beyond the iris radius in order to model the iris-loaded waveguide.

RESULTS & DISCUSSION

Bunching Comparison. Bunching for a reasonable current of 45 amps with and without an iris waveguide gives nearly identical results as expected (Fig. 3). The bunching maximum for both is near the predicted value given by the plasma approximation.

Achievable Bunching. Both types of space charge effects can be seen in the IFEL interactions. However, the importance is not in the type of compression and decompression that occurs, but the distance at which maximum compression occurs. Note that the maximum bunching is at about 0.4 m which is on the order of the theoretical 1.22 m calculated earlier. (See Fig. 3.) As current increases over the range from 45-1005 amps, the agreement between the
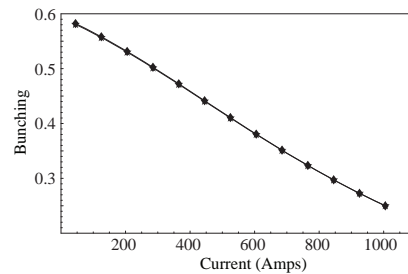
Figure 4: Simulated bunching, maximized at 0.4 m, as a function of current. Diamond indicates standard IFEL, star indicates iris IFEL.

bunching peak and the plasma length becomes much better. By 1005 amps, the theoretical plasma length is 0.259 m and maximum bunching occurs at approximately 0.243 m.

Of practical interest is the maximum bunching achievable at a measurable point in the experiment, which is in this case at 0.4 m. Bunching was maximized at this distance by adjusting power, for given currents. Again, both iris and standard IFEL profiles are nearly identical. (See Fig. 4.) For higher currents, the plasma oscillation dominates. A bunching maximum occurs earlier and at 0.4 m the bunching is decreased as it follows the plasma oscillation.

CONCLUSION

The data verifies the validity of an iris simulation using this method, as results closely match a non-iris situation, as expected. The simulation is then an early proof-of-concept for including an iris-loaded guide in an IFEL experiment. Iris-loaded guide scenarios must be tested more extensively in hopes of improving efficiency more dramatically. Longer IFEL/FEL experiments can be tested confidently using this approach. If efficiency is significantly improved in simulation, comparable real-world experiments can be performed as a final proof-of-concept. Increased efficiency in a proof-of-concept experiment would allow for application in generic IFEL/FEL processes and may prove to be a step toward practical applications of the technology.

REFERENCES

[1] J. Murphy, C. Pellegrini, Introduction to the Physics of the Free Electron Laser. Upton, NY. p. 163-216.

[2] S. Leone, Report of the Basic Energy Advisory Committee Panel on Novel Coherent Light Sources. 1999, University of Colorado.

[3] M. Xie, Laser Acceleration in Vacuum with an Open Iris-Loaded Waveguide. 1997, Lawrence Berkeley National Laboratory: Berkeley, CA.

[4] A. Siegman, *Lasers.* 1986, Sausalito, California: University Science Books.

[5] J. Rosenzweig, P. Musumeci, Phys. Rev., 1998. 58(3): p. R2738-R2740.

[6] S. Reiche, Nucl. Instr. & Meth. A429 (1999) 243